DOI: 10.61782/fa.2025.0968

FORUM ACUSTICUM
EURONOISE 2025

WAVE-BASED ANALYSIS OF FLANKING SOUND TRANSMISSION ACROSS JUNCTIONS WITH METAMATERIAL TREATMENT USING EFFECTIVE MEDIUM THEORY

Sofie Becuwe[1*] **Stijn Moons**[1,2] **Daniele Giannini**[1] **Edwin P. B. Reynders**[1]
[1] KU Leuven, Department of Civil Engineering, Structural Mechanics Section, Belgium
[2] CDM Stravitec, 3090 Overijse, Belgium

ABSTRACT

Reducing flanking sound transmission in buildings is challenging, with current options limited to mass increase and structural decoupling. This study explores an alternative approach using resonant metamaterial treatments, where small resonators are added on a subwavelength scale to the building elements connected via the junction. These offer a promising lightweight approach to achieve vibroacoustic attenuation, by creating wave propagation bandgaps that inhibit free-traveling waves within targeted frequency ranges. Wave propagation through the junctions is modeled using an analytical wave approach, in which thin isotropic semi-infinite plates are considered, and equilibrium and compatibility equations are imposed along the junction line. The metamaterial treatment is introduced in a computationally efficient way through effective medium theory, which locally employs homogenized material properties in the connected plates to capture the essential effects of subwavelength resonators. Results show that the structural transmission loss exhibits a significant increase close to the frequency of local resonance. To explore the achievable performance of the proposed treatments, various scenarios are analyzed, by varying the extent of the metamaterial treatment, from a narrow strip close to the junction to the full receiver plate, as well as the local resonator mass and multiple local resonances to address broader band effectiveness.

*__Corresponding author__: *sofie.becuwe@kuleuven.be.*

Keywords: *flanking sound transmission, wave-based analysis, locally resonant metamaterials, effective medium theory*

1. INTRODUCTION

Ensuring a sufficiently high level of sound insulation in buildings is a challenging problem, due to the presence of a multitude of sound transmission paths between the rooms across junctions of building elements, also called flanking transmission paths, through which vibrational energy is transmitted. Current solutions to suppress flanking paths involve mass increase and structural decoupling through elastic interlayers or linings, which however do not always prove to be feasible in renovations or lightweight constructions. To address these limitations, in this paper a new solution for the suppression of flanking sound is researched, based on resonant metamaterials.

Metamaterials are artificial structures, engineered to manipulate wave propagation on the microscopic (i.e., sub-wavelength) scale, such that at the macroscopic scale, an effective material is created with unconventional wave propagation properties that surpass those of conventional materials [1, 2]. Of the various types of metamaterials that have appeared over the years, resonant metamaterials (RMMs) are particularly attractive for noise control in buildings. By small resonators (periodically) added to a host structure on a subwavelength scale, RMMs achieve the suppression of free elastic wave propagation in a targeted frequency range [3, 4], while maintaining a light weight. Furthermore, by employing resonators that possess multiple resonances, known as multi-modal resonators, multiple frequency ranges can be targeted [5].

Recent developments make it possible to efficiently

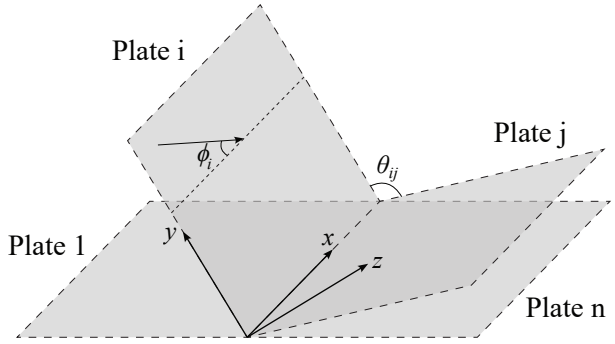

Figure 1: Schematic representation of a system of thin plates connected through a junction.

predict and quantify the influence of flanking sound transmission through junctions [6, 7], however these models only include the application of elastic interlayers, not RMMs. In this paper, the analytical model as described in [8] will therefore be expanded to include RMM applications too, by means of effective medium modeling [9]. With this technique, the effect of the subwavelength resonators is approximated by locally considering equivalent, frequency-dependent, material properties in the host structure [9].

The present paper is organized as follows. Section 2 summarizes the wave-based method to analyze flanking sound transmission across junctions, along with its extension through include RMM treatments. In Section 3, the method is used to analyze flanking transmission across a junction between two steel plates, for which different RMM treatments are considered by varying the width of the treated strip, the resonator mass, and the number of local resonances. Section 4 concludes the work.

2. METHODOLOGY

The used methodology consists of a combination of an analytical wave approach to model wave propagation through junctions [8] with effective medium theory to introduce the metamaterial treatment in a computationally efficient way as described in [9]. The considered system is a junction with n directly connected thin isotropic semi-infinite plates, each inclined at an angle θ_{ij} relative to an arbitrary reference plate (Fig. 1). The corresponding local coordinate system (x', y', z') for each plate is illustrated in Fig. 2. The metamaterial treatment can be applied both on the entire plate surface or a smaller strip close to the junction (Fig. 2). Due to both out-of-plane bending waves and in-plane longitudinal and shear waves, the plates vibrate.

The general aim is to determine the structural transmission coefficients τ_{ij}^{st} between an incident wave type s in plate i and a transmitted wave type t in plate j:

$$\tau_{ij}^{st}\left(\omega, \phi_i\right) := \frac{I_{\mathrm{y},j}^{t}}{I_{\mathrm{y},i}^{s}}. \tag{1}$$

with $I_{\mathrm{y},i}^{s}\left(\phi_i\right)$ the incident intensity and $I_{\mathrm{y},j}^{t}\left(\phi_i\right)$ the transmitted intensity in the local y'-direction per unit length of the connection. The transmission coefficient in Eq. (1) is dependent on the angle of incidence. The diffuse transmission coefficient, independent on the angle of incidence, for homogeneous isotropic plates, can be found as [6]:

$$\tau_{ij}^{st}\left(\omega\right) := \frac{1}{2}\int_0^{\pi} \tau_{ij}^{st}\left(\omega, \phi_i\right) \sin\phi_i \mathrm{d}\phi. \tag{2}$$

We here consider plane incident waves with incident angle $\phi_i = \operatorname{atan}\left(\frac{k_{\mathrm{y},i}^{s}}{k_{\mathrm{x}}}\right)$, frequency ω and wavenumbers k_{x} along the x-direction and k_{y} along the y-direction. Specifically, we consider only bending incident waves. This incident wave causes reflected and transmitted plane waves from the junction to each receiver plate j for any potential wave type t, which is considered to be a bending, shear or longitudinal wave. Compatibility at the junction imposes that the frequency ω and the wavenumber k_{x} along the x-direction, for all reflected and transmitted waves, are equal to the ones imposed by the incident wave.

The structural transmission loss in dB can subsequently be computed from the transmission coefficient as [10]:

$$R_{ij}\left(\omega\right) = -10\log\left(\tau_{ij}^{st}\left(\omega\right)\right). \tag{3}$$

The forces and displacements at the plate edge in the local coordinate system are illustrated in Fig. 2. From these, the incident and transmitted intensity can be computed as [11]:

$$I_{\mathrm{y},i}^{s}\left(\phi_i\right) := -\frac{\omega}{2}\mathrm{Im}\left(\mathbf{f}_{\mathrm{inc},i}^{s\mathrm{T}}\mathbf{u}_{\mathrm{inc},i}^{s*}\right), \tag{4}$$

$$I_{\mathrm{y},j}^{t}\left(\phi_i\right) := -\frac{\omega}{2}\mathrm{Im}\left(\mathbf{f}_{\mathrm{out},j}^{t\mathrm{T}}\mathbf{u}_{\mathrm{out},j}^{t*}\right), \tag{5}$$

with * denoting the complex conjugate. Specifically, the intensities for incident bending and transmitted bending

and in-plane longitudinal or shear waves are [8]:

$$I^{\mathrm{B}}_{\mathrm{y},i}\left(\phi_i\right) = -\frac{\omega}{2}\mathrm{Im}\left(f_{\mathrm{yz,inc},i}u^*_{\mathrm{z,inc},i} + m_{\mathrm{yy,inc},i}\theta^*_{\mathrm{x,inc},i}\right), \tag{6}$$

$$I^{\mathrm{B}}_{\mathrm{y},j}\left(\phi_i\right) = -\frac{\omega}{2}\mathrm{Im}\left(f_{\mathrm{yz,out},j}u^*_{\mathrm{z,out},j} + m_{\mathrm{yy,out},j}\theta^*_{\mathrm{x,out},j}\right), \tag{7}$$

$$I^{\mathrm{L/S}}_{\mathrm{y},j}\left(\phi_i\right) = -\frac{\omega}{2}\mathrm{Im}\left(f_{\mathrm{yx,out},j}u^*_{\mathrm{x,out},j} + f_{\mathrm{yy,out},j}u^*_{\mathrm{y,out},j}\right). \tag{8}$$

2.1 Plate model for plates without RMM treatment

In order to compute the forces and displacements in Eqs. (6) - (8) for plates without RMM treatment, the associated dynamic stiffness matrices need to be derived, which relate the forces and displacements at the plate edge. The plate edge displacements $\mathbf{u}_j\left(x', y', z', t\right)$ and forces per unit length $\mathbf{f}_j\left(x', y', z', t\right)$ for a plate j consist of contributions from the outgoing transmitted and reflected waves at the junction $\mathbf{u}_{\mathrm{out},j}$ and the incident wave $\mathbf{u}_{\mathrm{inc},j}$ [6]:

$$\mathbf{u}_j = \mathbf{u}_{\mathrm{out},j} + \mathbf{u}_{\mathrm{inc},j}, \tag{9}$$

$$\mathbf{f}_j = \mathbf{f}_{\mathrm{out},j} + \mathbf{f}_{\mathrm{inc},j}, \tag{10}$$

where $\mathbf{u}_{\mathrm{inc},j}$ and $\mathbf{f}_{\mathrm{inc},j}$ are only non-zero for the source plate.

The stiffness matrix $\mathbf{D}_j \in \mathbb{C}^{4x4}$ relating the forces $\mathbf{f}_{\mathrm{out},j}$ to the edge displacements $\mathbf{u}_{\mathrm{out},j}$, is composed of a contribution from the in-plane (IP) and out-of-plane (OOP) wave motion, represented respectively by $\mathbf{D}_{\mathrm{IP}}$ and $\mathbf{D}_{\mathrm{OOP}} \in \mathbb{C}^{2x2}$ [6]:

$$\underbrace{\begin{bmatrix} f_{\mathrm{yx}} \\ f_{\mathrm{yy}} \\ f_{\mathrm{yz}} \\ m_{\mathrm{yy}} \end{bmatrix}}_{:=\mathbf{f}_{\mathrm{out},j}} = \underbrace{\begin{bmatrix} \mathbf{D}_{\mathrm{IP}}\left(k_{\mathrm{x}}\right) & \mathbf{0} \\ \mathbf{0} & \mathbf{D}_{\mathrm{OOP}}\left(k_{\mathrm{x}}\right) \end{bmatrix}}_{\mathbf{D}_j\left(k_{\mathrm{x}}\right)} \underbrace{\begin{bmatrix} u_{\mathrm{x}}\left(y'=0\right) \\ u_{\mathrm{y}}\left(y'=0\right) \\ u_{\mathrm{z}}\left(y'=0\right) \\ \theta_{\mathrm{x}}\left(y'=0\right) \end{bmatrix}}_{\mathbf{u}_{\mathrm{out},j}}. \tag{11}$$

For compactness, the dependency from $\mathbf{D}_j$ on k_{x} is omitted in further equations. Eq. (11) can then be substituted into Eq. (10), resulting in the total force per unit length exerted by the plate on the junction:

$$\mathbf{f}_j = \mathbf{D}_j\mathbf{u}_{\mathrm{out},j} + \mathbf{f}_{\mathrm{inc},j}. \tag{12}$$

The stiffness matrices $\mathbf{D}_{\mathrm{IP}}$ and $\mathbf{D}_{\mathrm{OOP}}$ for in-plane and out-of-plane wave motion of isotropic plates can be computed according to [8]:

$$\mathbf{D}_{\mathrm{IP}}\left(k_{\mathrm{x}}\right) = \frac{Et}{k_{\mathrm{x}}^2 + k_{\mathrm{Sy}}k_{\mathrm{Ly}}}\begin{bmatrix} D_{11} & D_{12} \\ -D_{12} & D_{22} \end{bmatrix}, \tag{13}$$

with

$$D_{11} = -\frac{\mathrm{i}\left(k_{\mathrm{Sy}}^2 - k_{\mathrm{x}}^2\right)k_{\mathrm{Ly}}}{2\left(1+\nu\right)}, \tag{14}$$

$$D_{12} = \frac{\mathrm{i}\left(k_{\mathrm{Ly}}^2 + \nu k_{\mathrm{x}}^2\right)k_{\mathrm{x}}}{1-\nu^2} - \frac{\mathrm{i}k_{\mathrm{Sy}}k_{\mathrm{Ly}}k_{\mathrm{x}}}{1+\nu}, \tag{15}$$

$$D_{22} = -\frac{\mathrm{i}\left(\nu k_{\mathrm{x}}^2 + k_{\mathrm{Ly}}^2\right)k_{\mathrm{Sy}}}{1-\nu^2} - \frac{\mathrm{i}k_{\mathrm{x}}^2k_{\mathrm{Sy}}}{1+\nu}. \tag{16}$$

$$\mathbf{D}_{\mathrm{OOP}}\left(k_{\mathrm{x}}\right) = \frac{\mathrm{i}B}{k_{\mathrm{B1y}} - k_{\mathrm{B2y}}}\begin{bmatrix} D_{33} & D_{34} \\ D_{34} & D_{44} \end{bmatrix}, \tag{17}$$

with

$$B = \frac{Et^3}{12\left(1-\nu^2\right)}, \tag{18}$$

$$D_{33} = k_{\mathrm{B1y}}^3k_{\mathrm{B2y}} - k_{\mathrm{B2y}}^3k_{\mathrm{B1y}}, \tag{19}$$

$$D_{34} = \mathrm{i}k_{\mathrm{B2y}}^3 - \mathrm{i}k_{\mathrm{B1y}}^3 + \left(2-\nu\right)\left(k_{\mathrm{B2y}} - k_{\mathrm{B1y}}\right)\mathrm{i}k_{\mathrm{x}}^2, \tag{20}$$

$$D_{44} = k_{\mathrm{B2y}}^2 - k_{\mathrm{B1y}}^2, \tag{21}$$

where E is the Young's modulus, t the thickness of the plate, ν the Poisson's ratio and B the bending stiffness of the plate. k_{B1y}, k_{B2y}, k_{Ly} and k_{Sy} can be found from the equations of motion for OOP and IP motion and are dependent on k_{x} and the bending, longitudinal and shear wavenumbers, given by:

$$k_{\mathrm{B},j} = \left(\frac{\rho_{\mathrm{OOP},j}t_j\omega^2}{B_j}\right)^{1/4}, \tag{22}$$

$$k_{\mathrm{L},j} = \sqrt{\frac{\rho_{\mathrm{IP},j}(1-\nu_{\mathrm{IP},j})^2\omega^2}{E_{\mathrm{IP},j}}}, \tag{23}$$

$$k_{\mathrm{S},j} = \sqrt{\frac{2\rho_{\mathrm{IP},j}(1+\nu_{\mathrm{IP},j})\omega^2}{E_{\mathrm{IP},j}}}. \tag{24}$$

In the case of plates without RMM treatment, the mass densities $\rho_{\mathrm{OOP},j}$ and $\rho_{\mathrm{IP},j}$ are both frequency-independent.

Subsequently, the forces and moment equilibrium and displacement compatibility are imposed at the junction line. The equations are expressed in the global coordinate system, denoted with subscript g, with a transformation matrix $\mathbf{R}_j$ [6]:

$$\mathbf{u}_{\mathrm{g}} = \mathbf{R}_j\mathbf{u}_j, \tag{25}$$

$$\mathbf{f}_{\mathrm{g},j} = \mathbf{R}_j\mathbf{f}_j = \mathbf{R}_j\mathbf{D}_j\mathbf{R}_j^{-1}\mathbf{u}_{\mathrm{g}}, \tag{26}$$

where

$$\mathbf{R}_j := \begin{bmatrix} 1 & 0 & 0 & 0 \\ 0 & \cos\theta_{ij} & -\sin\theta_{ij} & 0 \\ 0 & \sin\theta_{ij} & \cos\theta_{ij} & 0 \\ 0 & 0 & 0 & 1 \end{bmatrix}. \tag{27}$$

For the source plate, $\theta_{ij} = 0$, while for the receiver plate, θ_{ij} is equal to the angle between the source and receiver plate. The displacements and forces exerted on the junction by an incident bending wave are then found as [8]:

$$\mathbf{u_{inc}} = \begin{bmatrix} u_\mathrm{x} \\ u_\mathrm{y} \\ u_\mathrm{z} \\ \theta_\mathrm{x} \end{bmatrix} = \begin{bmatrix} 0 \\ 0 \\ u_{\mathrm{z,inc}} \\ \theta_{\mathrm{x,inc}} \end{bmatrix}, \tag{28}$$

$$\mathbf{f_{inc}} = \begin{bmatrix} f_{\mathrm{yx}} \\ f_{\mathrm{yy}} \\ f_{\mathrm{yz}} \\ m_{\mathrm{yy}} \end{bmatrix} = \begin{bmatrix} 0 \\ 0 \\ f_{\mathrm{yz,inc}} \\ m_{\mathrm{yy,inc}} \end{bmatrix}, \tag{29}$$

with $u_{\mathrm{z,inc}} = \alpha_i$, $\theta_{\mathrm{x,inc}} = i\alpha_i k_y$, $f_{\mathrm{yz,inc}} = -\alpha_i B_1(k_y^3 - (2-\nu_{1\mathrm{OOP}})k_x^2 k_y)$ and $m_{\mathrm{yy,inc}} = \alpha_i B_1(k_y^2 - \nu_{1\mathrm{OOP}} k_x^2)$. α_i represents the amplitude of the incident wave, here taken equal to unity. The incident wave power in the y-direction then becomes [6]:

$$I_\mathrm{inc} = \frac{\rho_{1\mathrm{OOP}} t_1 \omega^3 \alpha^2}{k_{\mathrm{B1}}} \sin\phi_i. \tag{30}$$

In the next step, the equilibrium equation can be rewritten for n plates with a source plate i as the sum of the forces from Eq. (12) exerted by all plates [8]:

$$\sum_{j=1}^{n} \mathbf{f}_{\mathrm{g},j} = \mathbf{0}, \tag{31}$$

$$\sum_{j=1}^{n} \mathbf{R}_j \mathbf{D}_j \mathbf{u}_j = \mathbf{R}_i \left(\mathbf{D}_i \mathbf{u}_\mathrm{inc} - \mathbf{f}_\mathrm{inc}\right). \tag{32}$$

Taking into account the compatibility requirements at the junction, Eq. (25) is substituted into this expression:

$$\left(\sum_{j=1}^{n} \mathbf{R}_j \mathbf{D}_j \mathbf{R}_j^\mathrm{T}\right) \mathbf{u}_\mathrm{g} = \mathbf{R}_i \left(\mathbf{D}_i \mathbf{u}_\mathrm{inc} - \mathbf{f}_\mathrm{inc}\right). \tag{33}$$

Eq. (33) is solved for the displacements $\mathbf{u}_\mathrm{g}$ at the junction. The displacements for every receiver plate j in the local coordinate system can then be found as:

$$\mathbf{u}_j = \mathbf{R}_j^\mathrm{T} \mathbf{u}_{\mathrm{g},j}. \tag{34}$$

From this result, $\mathbf{u}_{\mathrm{out},j}$ can be computed as $\mathbf{u}_j - \mathbf{u}_\mathrm{inc}$ when the considered plate contains the incident wave. Otherwise, $\mathbf{u}_{\mathrm{out},j}$ is equal to $\mathbf{u}_j$. The related forces can be found as $\mathbf{f}_{\mathrm{out},j} = \mathbf{D}_j \mathbf{u}_{\mathrm{out},j}$. In that way, all the input values for Eqs. (6)-(8) are determined.

2.2 Plate-strip model for plates with RMM treatment

To reduce flanking sound transmission through junctions, RMMs can be applied to a full plate or only in a strip close to the junction. When plates are fully treated with RMMs, the same methodology as described in Section 2.1 can be applied, with only one difference: in that case the mass density in Eq. (22) is not frequency-independent anymore. Due to the resonators, the OOP mass density will be influenced by inertial contributions of each resonator mode k. This results in an effective mass density, taking into account the modal effective masses. The effective mass density of a multi-modal metamaterial panel is obtained as [9]:

$$\rho_{\mathrm{eff,z}}(\omega) = \rho + \frac{1}{t} \sum_{k=1}^{n_\mathrm{m}} \frac{m''_{\mathrm{z},k}(1+\mathrm{i}\eta)}{(1+\mathrm{i}\eta) - (\omega/\omega_k)^2}, \tag{35}$$

with ρ the mass density of the host plate, n_m the modes of interest, t the thickness of the host plate, $m''_{\mathrm{z},k}$ the modal effective translational masses, η the damping loss factor of the resonators and ω_k the fixed base natural frequencies of the resonator.

If only a RMM strip close to the junction is considered, this strip has a frequency-dependent OOP effective mass density, while the OOP mass density of the untreated connected plate is frequency-independent. The IP mass density is always frequency-independent, but due to the added resonators, an additional static mass needs to be added to the mass density of the host structure. To include the effect of a RMM strip between the junction and an untreated connected plate, the prediction model as described in section 2.1 needs to be expanded, following the methodology developed in [7, 8] for thin plate interlayers. Contrary to the previously considered plates, the RMM strip has a finite dimension in the y'-direction. Thus not only the displacements and forces at the junction line (2) need to be taken into account, but also the forces and displacements at the interface between the RMM strip and the connected plate (1), as illustrated in Fig. 2. The relation between the forces per unit length $\mathbf{f}_\mathrm{l}$ and the displacements $\mathbf{u}$ at both endplanes of the RMM strip can be expressed in the local coordinate system through a stiff-

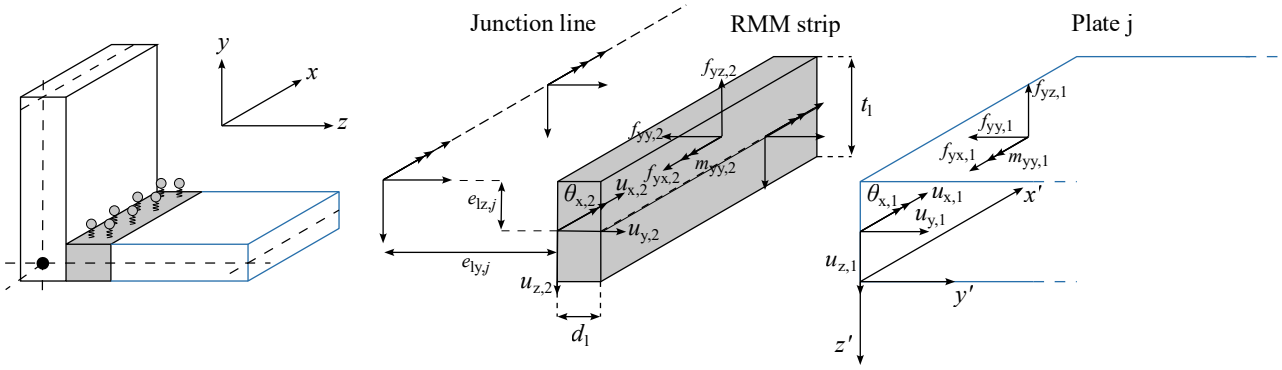

Figure 2: Exploded view of a plate/strip system.

ness matrix $\mathbf{D}_\mathrm{l}$ [8]:

$$\mathbf{f}_\mathrm{l} = \mathbf{D}_\mathrm{l}\,\mathbf{u}, \tag{36}$$

where

$$\mathbf{f}_\mathrm{l} := [\mathbf{f}_{\mathrm{l},1} \;\; \mathbf{f}_{\mathrm{l},2}]^\mathrm{T} = [\mathbf{f}_\mathrm{l}\,(y'=d_\mathrm{l}) \;\; \mathbf{f}_\mathrm{l}\,(y'=0)]^\mathrm{T}, \tag{37}$$

$$\mathbf{u} := [\mathbf{u}_1 \;\; \mathbf{u}_2]^\mathrm{T} = [\mathbf{u}\,(y'=d_\mathrm{l}) \;\; \mathbf{u}\,(y'=0)]^\mathrm{T}. \tag{38}$$

For each plate j connected to the junction through a RMM strip, the exerted forces $\mathbf{f}_{1,j}$ at position (1) and $\mathbf{f}_{2,j}$ at position (2) can be divided into a direct contribution from the plate $\mathbf{f}_{\mathrm{p},j}$ as in Eq. (11) and a contribution related to the RMM strip itself $\mathbf{f}_{\mathrm{l},j}$ [8]:

$$\mathbf{f}_j = \mathbf{f}_{\mathrm{p},j} + \mathbf{f}_{\mathrm{l},j}, \tag{39}$$

$$\mathbf{f}_{\mathrm{g},j} = \mathbf{D}_{\mathrm{g,p},j}\mathbf{u}_\mathrm{g} + \mathbf{D}_{\mathrm{g,l},j}\mathbf{u}_\mathrm{g}, \tag{40}$$

where the subscript g denotes the global coordinate system and

$$\mathbf{D}_{\mathrm{g,p},j} = \begin{bmatrix} \mathbf{R}_j\mathbf{D}_j\mathbf{R}_j^\mathrm{T} & \mathbf{0} \\ \mathbf{0} & \mathbf{0} \end{bmatrix}, \tag{41}$$

$$\mathbf{D}_{\mathrm{g,l},j} = \begin{bmatrix} \mathbf{R}_\mathrm{j} & \mathbf{0} \\ \mathbf{0} & \mathbf{R}_{\mathrm{l},j} \end{bmatrix} \underbrace{\begin{bmatrix} \mathbf{D}_{\mathrm{l},j,11} & \mathbf{D}_{\mathrm{l},j,12} \\ \mathbf{D}_{\mathrm{l},j,21} & \mathbf{D}_{\mathrm{l},j,22} \end{bmatrix}}_{\mathbf{D}_{\mathrm{l},j}} \begin{bmatrix} \mathbf{R}_j^\mathrm{T} & \mathbf{0} \\ \mathbf{0} & \mathbf{R}_{\mathrm{l},j}^\mathrm{T} \end{bmatrix}, \tag{42}$$

with $\mathbf{D}_j$ being the dynamic stiffness matrix for a thin plate j as in Eqs. (13) and (17). The stiffness matrix $\mathbf{D}_{\mathrm{l},j}$ of a RMM strip consists of four block matrices $\mathbf{D}_{\mathrm{l},j,mn} \in \mathbb{C}^{4x4}$. The strip is considered as a waveguide, in contrary to the two steel plates which are considered as halfspaces. Due to the finite y'-dimension, waves in both the positive and negative y'-direction are considered for the deformation of the layer. The stiffness matrices can be computed in a similar way as in section 2.1, and can be found in [8].

Since the endplane of the RMM strip could have offsets $e_{\mathrm{ly},j}$ and $e_{\mathrm{lz},j}$ relative to the theoretical junction line, as illustrated in Fig. 2, the transformation matrix (27) needs to be adapted for the RMM strip as [8]:

$$\mathbf{R}_{\mathbf{l,j}} := \begin{bmatrix} 1 & 0 & 0 & 0 \\ 0 & \cos\theta_{ij} & -\sin\theta_{ij} & 0 \\ 0 & \sin\theta_{ij} & \cos\theta_{ij} & 0 \\ 0 & e_{\mathrm{lz},j} & e_{\mathrm{ly},j} & 1 \end{bmatrix}. \tag{43}$$

where the transformation matrix (27) corresponded to the situation in which these offsets are zero.

The global force equilibrium per unit length is then evaluated both at the junction line and at each interface between a RMM strip and at its connected plate:

$$\sum_{j=1}^{n} \mathbf{f}_{\mathrm{g1},j} = \begin{cases} \mathbf{R}_i\,(\mathbf{D}_i\mathbf{u}_\mathrm{inc} - \mathbf{f}_\mathrm{inc}), & \text{if } j = i \\ \mathbf{0}, & \text{if } j \neq i \end{cases} \tag{44}$$

$$\sum_{j=1}^{n} \mathbf{f}_{\mathrm{g2},j} = \begin{cases} \mathbf{0}, & \text{if } j = i \\ \mathbf{R}_i\,(\mathbf{D}_i\mathbf{u}_\mathrm{inc} - \mathbf{f}_\mathrm{inc}), & \text{if } j \neq i \end{cases} \tag{45}$$

3. APPLICATION

In this Section, the methodology described in Section 2 is applied to a rigidly connected horizontal junction of steel plates, where both fully treated RMM plates and plates with only a small RMM strip close to the junction are considered. The results are compared with the junction models without any RMM treatment, to quantify the attenuation provided by RMM treatments on flanking sound transmission.

The steel plates without RMM treatment are considered isotropic and so the OOP and IP properties are the

same. The properties of the considered steel plates are: $\rho = 7850$ kg/m^3, $E = 210 \cdot 10^9$ Pa, $t = 0.002$ m, $\nu = 0.3$. From these parameters, the surface mass, shear modulus and bending stiffness can be computed as $m = \rho t$, $G = E/2(1+\nu)$ and $B = Et^3/12(1-\nu^2)$ respectively.

A distinction is made between OOP and IP material properties for the parts of the structure with RMM treatment. The IP properties remain the same as for the untreated plate, except for the mass density, where an additional static mass is added due to the presence of the resonators. In this paper, the added static mass due to the resonators will be initially taken equal to 10% of the mass of the host structure belonging to one resonator. The OOP mass density can be found through effective medium modeling with Eq. (35). The resonance frequency of the resonators is set to 500 Hz.

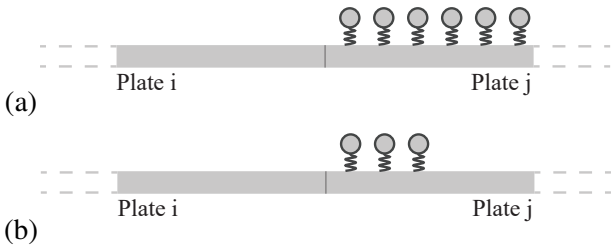

Figure 3: Junction between two plates ($\theta_{ij} = \pi$) with a fully treated RMM receiver plate (a) and with a treated RMM strip close to the junction (b).

3.1 Fully treated receiver plate

The first case we consider, is a junction of two steel plates of which the receiver plate is fully treated with resonators, as illustrated in Fig. 3a. The source plate i is further denoted as plate 1, the receiver plate j as plate 2.

The structural transmission loss for the transmitted bending waves is shown in Fig. 4 for a junction between two plates with an angle $\theta_{12} = \pi$. The receiver plate is fully treated with resonators with a damping of 0 and a local resonator mass of 10 % and 20 % with respect to the mass of the host plate. The structural transmission coefficient for longitudinal and shear waves is very small with respect to the transmission coefficient for bending waves, and therefore the structural transmission loss for these wave-types is not further considered in this paper. The graphs show that due to the RMM treatment of the receiver plate, at the resonance frequency of 500 Hz, less vibrational energy is transmitted from the source into the receiver plate and so the RMM treatment is effective to reduce wave propagation at the targeted frequency.

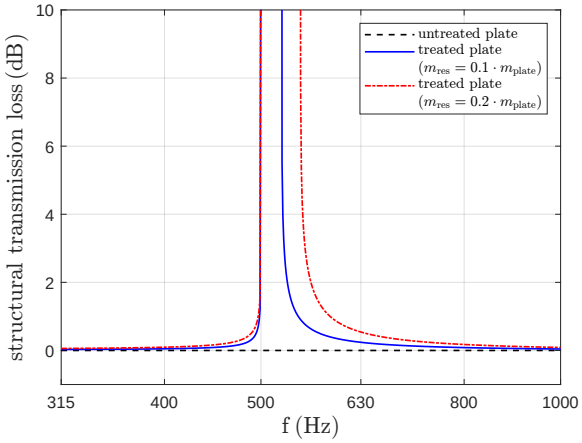

Figure 4: Comparison between the structural transmission loss for the transmitted bending waves through a junction ($\theta_{12} = \pi$) with an untreated and fully treated receiver plate with no damping in the resonators and a local resonator mass of 10 % and 20 % with respect to the mass of the host plate.

3.2 Influence of the local resonator mass

In a second case, the influence of the added resonator mass with respect to the host structure is analyzed, which is also shown in Fig. 4. In a first case, the local resonator mass is taken to be 10 % of the mass of the host structure. In a second case, the local resonator mass is taken to be 20 % of the mass of the host structure. The graphs in Fig. 4 show that in the case of 20 % added mass, the bandgap that inhibit free-traveling waves at the resonance frequency of the resonators widens, resulting in a broader frequency range in which the transmitted vibrational energy is reduced. Even though not shown here, similar results have been obtained for another resonator damping, other angles θ_{12} of the junction and in the case only a strip of resonators is applied.

3.3 Receiver plate with RMM strip

Thirdly, only a small strip of resonators is applied close to the junction, as illustrated in Fig. 3b. The strip is modeled as a part of the junction as discussed in Section 2.2,

and so the structural transmission loss is computed for the transmitted bending waves after the strip. The results are shown in Fig. 5 for a junction between two plates with an angle $\theta_{12} = \pi$, with a resonator damping of 0 (Fig. 5a) and 0.02 (Fig. 5b). The results are shown for a strip with a width of 0.03 m, 0.05 m, 0.10 m, 0.15 m and 0.3 m. From these graphs it is clear that we can achieve already a significant reduction in wave propagation from source to receiver plate at the resonance frequency by applying only a small strip of resonators close to the junction. Fig. 5a shows that the frequency range in which free wave propagation is inhibited becomes larger by increasing the width of the strip. From Fig. 5b it is clear that the larger the width of the strip is, the larger the structural transmission loss through the RMM strip will be. Similar results are obtained for another resonator damping and other angles θ_{12} of the junction. When a strip of resonators with very low damping is considered, additional drops in the structural transmission loss are visible, caused by Fabry-Perot standing waves. However, this is only significant at very low damping values, and thus has no impact in practice.

3.4 Influence of multi-modal resonators

As a fourth case, the influence of multi-modal resonators is examined. Multi-modal resonators allow to have multiple resonance frequencies, resulting in broader band effectiveness. As an example, a junction with an angle $\theta_{12} = \pi$ is considered, with a treated strip of 0.15 m close to the junction in the receiver plate and a damping of 0, 0.02, 0.05 or 0.1 in the resonators. Three resonance frequencies (500 Hz, 460 Hz, 420 Hz) are considered. The results are shown in Fig. 6. A peak is visible at each resonance frequency of the multi-modal resonator, resulting in a more broadband reduction of the transmitted vibrational energy. Even though not shown here, similar results have been obtained for another resonator damping, other angles θ_{12} of the junction and in the case a fully treated receiver plate is applied.

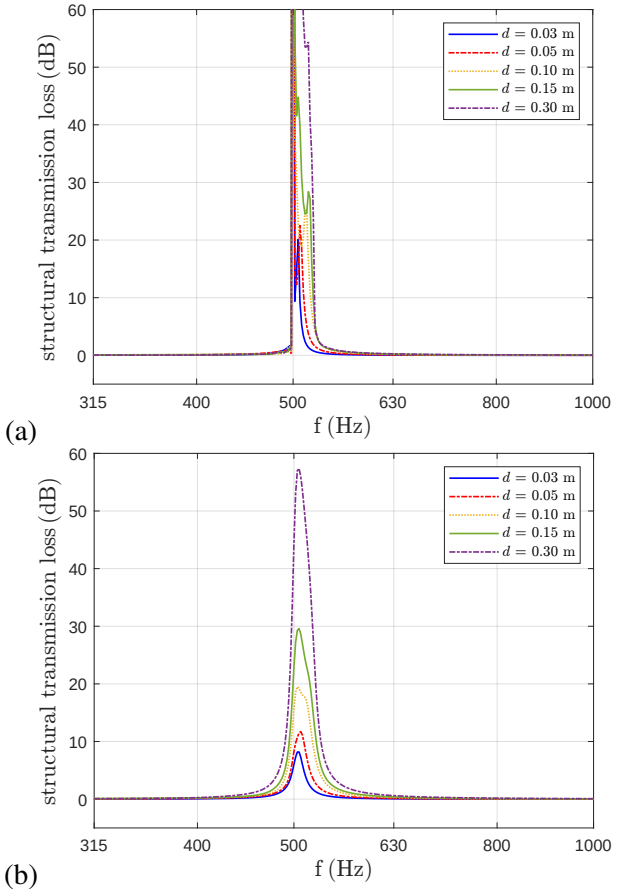

Figure 5: Comparison of the structural transmission loss for the transmitted bending waves between a junction ($\theta_{12} = \pi$) with a treated strip close to the junction in the receiver plate for a damping of 0 (a) and 0.02 (b) in the resonators. Results are shown for a strip width of 0.03 m, 0.05 m, 0.10 m, 0.15 m and 0.3 m.

4. CONCLUSION

In this paper, an analytical wave approach to model wave propagation through junctions was combined with effective medium theory to introduce a metamaterial treatment in the junction design. The proposed model has been used to study flanking transmission across junctions with steel plates, exploring various scenarios in which the width of the treated strip, the resonator mass, and the number of local resonances were changed. Varying the width of the metamaterial strip has proven that already a significant reduction in wave propagation can be obtained for sufficiently wide strips. Increasing the mass of the local resonators broadens the frequency range in which bending wave transmission to the receiver plate is reduced, but it can however conflict with lightweight requirements. Another way of widening the band of effectiveness is therefore to use multi-modal resonators, allowing to include multiple resonance frequencies. The methodology proposed in this work sets a framework to analyze and de-

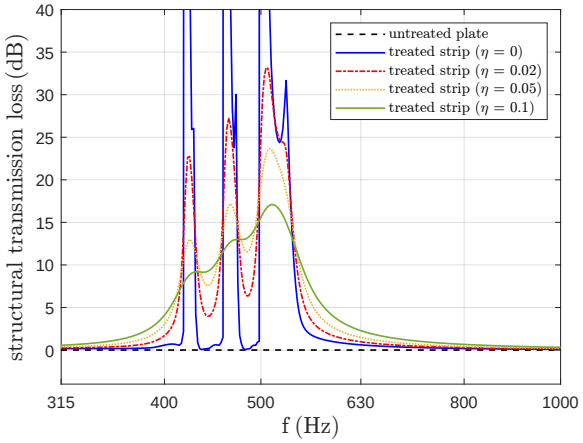

Figure 6: Comparison of the structural transmission loss for the transmitted bending waves through a junction ($\theta_{12} = \pi$) with a treated strip of 0.15 m close to the junction in the receiver plate, for a damping of 0, 0.02, 0.05 and 0.1 in the resonators. Three resonance frequencies (500 Hz, 460 Hz, 420 Hz) are considered.

sign metamaterial treatments for the suppression of flanking sound transmission across junctions of plates. Future research will focus on further validation against numerical and experimental results for practical applications.

5. ACKNOWLEDGMENTS

The presented research has been performed within the framework of the project "Resonant metamaterials for broadband suppression of flanking sound transmission in buildings" (Grant 1S38725N), funded by the Research Foundation Flanders (FWO), Belgium. Stijn Moons gratefully acknowledges the financial support of Flanders Innovation & Entrepreneurship (VLAIO) through the Baekeland fellowship HBC.2022.0712. Daniele Giannini gratefully acknowledges the financial support of the Research Foundation Flanders (FWO) through the postdoctoral fellowship 12A3Q24N.

6. REFERENCES

[1] M. Hussein, M. Leamy, and M. Ruzzene, "Dynamics of phononic materials and structures: historical origins, recent progress, and future outlook," *Applied Mechanics Reviews*, vol. 66, no. 4, pp. 040802–3, 2014.

[2] G. Ma and P. Sheng, "Acoustic metamaterials: From local resonances to broad horizons," *Science Advances*, vol. 2, no. 2, p. e1501595, 2016.

[3] F. Lemoult, N. Kaina, M. Fink, and G. Lerosey, "Wave propagation control at the deep subwavelength scale in metamaterials," *Nature Physics*, vol. 9, pp. 55–60, 2013.

[4] C. Claeys, K. Vergote, P. Sas, and W. Desmet, "On the potential of tuned resonators to obtain low-frequency vibrational stop bands in periodic panels," *Journal of Sound and Vibration*, vol. 332, no. 6, pp. 1418–1436, 2013.

[5] D. Giannini, M. Schevenels, and E. Reynders, "Rotational and multimodal local resonators for broadband sound insulation of orthotropic metamaterial plates," *Journal of Sound and Vibration*, vol. 547, no. 117453, pp. 1–17, 2023.

[6] R. Langley and K. Heron, "Elastic wave transmission through plate/beam junctions," *Journal of Sound and Vibration*, vol. 143, no. 2, pp. 241–253, 1990.

[7] P. Mees and G. Vermeir, "Structure-borne sound transmission at elastically connected plates," *Journal of Sound and Vibration*, vol. 166, no. 1, pp. 55–76, 1993.

[8] S. Moons, R. Lanoye, and E. Reynders, "Prediction of flanking sound transmission through cross-laminated timber junctions with resilient interlayers," *Applied Acoustics*, vol. 228, no. 110317, pp. 1–15, 2025.

[9] D. Giannini and E. Reynders, "Effective medium modelling of real-world multi-modal metamaterial panels achieving broadband vibroacoustic attenuation," *Extreme Mechanics Letters*, vol. 69, p. 102161, 2024.

[10] R. Craik, *Sound transmission through buildings using statistical energy analysis*. Aldershot, UK: Gower, 1996.

[11] L. Cremer and M. Heckl, *Structure-borne sound: Structural vibrations and sound radiation at audio frequencies*. Berlin: Springer, 2nd ed., 1988.